Main Manuscript for

Retrospective Attention Can Trigger Visual Perception Without Dependence on Either Cue Awareness or Target Reporting.

Ye Li1,2,3, Xingbei Wan1,2, Mingxing Mao1,2, Lingying Jin1,2, Xilin Zhang1,2

1 Key Laboratory of Brain, Cognition and Education Sciences, Ministry of Education, South China Normal University, Guangzhou, Guangdong 510631, China

2 School of Psychology, Center for Studies of Psychological Application, Guangdong Provincial Key Laboratory of Mental Health and Cognitive Science, South China Normal University, Guangzhou, Guangdong 510631, China

3 Lead contact

* Ye Li

Email: yeli.academic@gmail.com

PNAS strongly encourages authors to supply an ORCID identifier for each author. Do not include ORCIDs in the manuscript file; individual authors must link their ORCID account to their PNAS account at www.pnascentral.org. For proper authentication, authors must provide their ORCID at submission and are not permitted to add ORCIDs on proofs.

Author Contributions: Paste the author contributions here.

Competing Interest Statement: Disclose any competing interests here.

Classification: Paste the major and minor classification here. Dual classifications are permitted, but cannot be within the same major classification.

Keywords: Paste the keywords here. There should be at least three and no more than five.

This PDF file includes:

Main Text
Figures 1 to X
Tables 1 to X

Abstract

The interplay between attention and visual consciousness remains pivotal in cognitive neuroscience, framed by three hypotheses: dual dissociation (independent mechanisms), single dissociation (consciousness requires attention but not vice versa), and interdependence (bidirectional coupling). We tested these through retrospective attention—a bottom-up post-stimulus mechanism—to clarify its role in visual awareness.

Three EEG experiments combined backward masking and no-report paradigms to assess retrospective attention's effects on Gabor patch discrimination. Experiments 1&2 showed invisible retro-cues enhanced orientation discrimination at 66.67 ms SOA (via N2pc modulation), while visible cues sustained effects up to 100 ms. Experiment 3 revealed explicit reporting amplified

P3b and attenuated Visual Awareness Negativity (VAN), whereas no-report conditions retained contrast-driven VAN without P3b modulation. Multivariate decoding linked report-dependent attention to frontoparietal networks with temporally generalized activity, while no-report effects localized to parieto-occipital regions, enhancing awareness decoding at high contrast.

Results support the single dissociation hypothesis: retrospective attention enhances perception independently of cue awareness and reporting, yet flexibly modulates both access (report-linked P3b) and phenomenal consciousness (contrast-dependent VAN). This study provides the first neural evidence for unconscious retrospective attention, extends the global neuronal workspace theory by dissociating report-dependent/independent processes, and clarifies temporal dynamics in awareness formation. By distinguishing phenomenal and access consciousness, we establish attention's critical role in mediating visual awareness, advancing cognitive neuroscience frameworks.

Significance Statement

This study reveals that unconscious retrospective attention enhances visual perception independently of explicit reporting, challenging traditional views that attention requires consciousness. By dissociating neural mechanisms of phenomenal (subjective experience) and access consciousness (reportable awareness), we demonstrate attention's dual role in modulating both processes. Our findings extend the global neuronal workspace theory, provide the first neural evidence for unconscious retroactive attentional effects, and clarify how attentional mechanisms temporally shape awareness. Methodologically, integrating no-report paradigms with multivariate decoding advances consciousness research by minimizing reporting biases. These insights bridge theoretical debates in cognitive neuroscience and inform clinical approaches to consciousness disorders and AI models of visual processing.

Main Text

Introduction

Visual perception is shaped by dynamic interactions between sensory processing and attentional modulation. A critical question emerging in consciousness research is whether retrospective attention—post-stimulus cueing—can reactivate sensory traces and retroactively influence conscious perception (1, 2). This phenomenon challenges traditional models of perception by suggesting that conscious awareness operates within an extended temporal window, where post-perceptual attentional mechanisms refine sensory representations (3, 4).

Recent studies confirm that retro-cues enhance perceptual discrimination (2, 5), with effects attributed to either sensory reactivation (5) or attentional amplification (1).These findings align with the Global Neuronal Workspace Theory (GNWT), which posits that conscious access depends on the global broadcast of sensory information via attentional mechanisms (6). However, debates persist regarding confounding factors such as working memory (7, 8) and the role of exogenous attention in driving these effects. Notably, Xia et al. (5) demonstrated that local visual interactions alone can elicit retro-perception effects, challenging the necessity of attentional mediation.

The neural mechanisms underlying these effects remain unresolved, particularly given competing theories of consciousness-attention relationships: Dual dissociation: Attention and consciousness rely on independent neural substrates (9); Single dissociation: Consciousness requires attentional amplification, while attention operates unconsciously (10); Mutual dependency: Bidirectional modulation through dynamic coupling (11). To address these controversies, we combined two paradigms: Backward masking (12) to isolate subliminal sensory interactions. No-report protocols (13) to minimize post-perceptual confounds. We further employed EEG to track neural correlates of consciousness (NCCs; e.g., VAN, P3b) and attention (e.g., N2pc, alpha-band modulation). Three hypotheses were tested: Sensory-mediated retro-perception persists under backward masking, independent of cue awareness. Retro-cue effects enhance NCCs even without explicit

reporting, supporting GNWT's prediction of attention-dependent conscious access. Dissociable neural signatures distinguish attentional vs. sensory retro-perception mechanisms.
This study advances the field by: Resolving debates about the necessity of attention in retro-perception. Providing the first neurophysiological evidence for retro-cue mechanisms. Testing consciousness theories (GNWT, RPT) in a novel temporal context. By integrating behavioral, neural, and theoretical approaches, we clarify how post-perceptual processes shape conscious experience, offering insights into the temporal flexibility of visual awareness.

Results

Experiment 1

We investigated whether unconscious exogenous post-cue attention could modulate the perception of a single threshold-level stimulus. Participants performed an orientation discrimination task on a briefly presented low-contrast Gabor patch (calibrated to 75% baseline accuracy) while exogenous attention was cued by a dimming circle either before (pre-cue) or after (post-cue) the target. Critically, the dimming cue minimized masking interference with the target. A two-alternative forced-choice (2AFC) task was used to assess both orientation discrimination (primary task) and cue location awareness (control task) (Figure 1A). Participants were required to report the target's orientation, with contrast individually calibrated to 75% baseline accuracy. Attention was cued by a brief dimming of a circle either before (pre-cue) or after (post-cue) the target, followed by an 83.33 ms mask (invisible condition) or fixation period (visible condition). Cue visibility was verified in a 2AFC task: visible cues achieved 98.30% (±2.86%) accuracy, while invisible cues were at chance level (49.39% ±2.68%, chance = 50%; Figure 1B).
When cues were unmasked (visible), we replicated the classic time course of exogenous attention (Figure 1B). A two-way ANOVA [Congruency (valid/invalid) × SOA (-116.67 ms, +66.67 ms, +100 ms)] revealed a significant main effect of congruency [$F(1,23) = 111.64$, $P < 0.001$], with valid cues (same side as target) enhancing orientation accuracy compared to invalid cues (opposite side). Crucially, this facilitation persisted even when cues were presented after target offset. Bonferroni-corrected post-hoc comparisons confirmed significant validity effects across all SOAs (all corrected $P < 0.001$), including the +100 ms condition where valid cues still improved performance relative to the 75% baseline (Figure 1B).
Under masked (invisible cue) conditions, attentional effects were reduced but remained significant [validity main effect: $F(1,23) = 16.33$, $P = 0.001$]. Post-hoc tests confirmed validity effects at -116.67 ms ($P_{corrected} = 0.022$) and +66.67 ms SOAs ($P_{corrected} = 0.015$), but not at +100 ms ($P_{corrected} = 0.257$;Figure 1D).
These results indicate that directing attention to a target's location after its disappearance enhances orientation discrimination even when cues are invisible, suggesting local sensory interactions rather than post-perceptual processing. The disappearance of this effect at +100 ms SOA under invisible cues highlights its strict temporal constraints.

Experiment 2

Behavior Results

This second experiment, including 22 new volunteers, was similar to the previous one except that the SOA between the target and the cue was fixed at 66.67 ms; a Non-cue condition was added to the cue presentation; and only the mask stimulus was presented, thereby maintaining only the invisible condition. Results on the objective orientation discrimination task replicated the results of the first experiment (Figure 1F) [congruency: $F(1,20) = 5.66$, $P = 0.011$]. Post-hoc comparisons with BONFERRONI correction indicated significant differences between valid and invalid cues ($P_{corrected} = 0.002$), but not between valid and non-cue conditions ($P_{corrected} = 0.169$).

EEG Results

The N2pc in the report and no-report conditions in experiment 2

Results from the N2pc analysis are shown in Figure 2. N2pc amplitudes significantly differed between the contralateral and ipsilateral ectrodes across the three congruency conditions [ANOVA with factors congruency (valid/invalid/no-cue, 3) × electrodes (ipsilateral/contralateral, 2): $F(2, 20) = 2.264$, $P = 0.129$; electrodes: $F(1, 22) = 30.39$, $P < 0.001$]. Post-hoc comparisons with

BONFERRONI correction indicated significant differences between contralateral and ipsilateral electrodes in all three congruency conditions (Figure 2A, valid, $P_{corrected} < 0.001$; Figure 2B, invalid, $P_{corrected} = 0.006$; Figure 2C, no-cue, $P_{corrected} < 0.001$). N2pc difference wave amplitudes (contralateral minus ipsilateral) significantly differed between the valid, non-cue, and invalid conditions [ANOVA with factors congruency (valid/invalid/non-cue, 3): $F(2, 20) = 14.76$, $P_{corrected} < 0.001$]. Post-hoc comparisons with BONFERRONI correction indicated significant differences not only between valid and invalid conditions but not between valid and non-cue conditions (valid versus invalid, $P_{corrected} = 0.025$; valid versus non-cue, $P_{corrected} = 0.231$; invalid versus non-cue, $P_{corrected} = 0.029$). The results showed that even under conditions where the cue was invisible, post-cue attention could still modulate the classic attention-related ERP component N2pc.

Experiment 3

Behavior results

This third experiment, involving 20 new participants, was similar to the first experiment but with several key modifications. The stimulus onset asynchrony (SOA) between the target and the cue was fixed at 66.67 ms. Only the fixation stimulus was presented, maintaining the visible condition. Two circles were positioned above and below the fixation point, with the Gabor patch and the cue randomly appearing in one of these circles (Figure 3A).

A significant addition was the introduction of three Gabor contrast levels for the target presentation. These contrast levels followed a linear growth pattern (Figure 3B), with average values of 0.00662 (Low), 0.01845 (Medium), and 0.03088 (High), and standard deviations of 0.00367 (Low), 0.00598 (Medium), and 0.00873 (High).

In the report task, the results of the orientation discrimination task successfully replicated the findings of Experiment 1 [congruency effect: $t(1, 19) = 84.67$, $P_{corrected} < 0.001$] (Figure 3C). Bonferroni-corrected post-hoc comparisons revealed significant differences between valid and invalid cue conditions at medium-contrast ($P_{corrected} = 0.002$) and high-contrast ($P_{corrected} = 0.014$) levels. However, no significant difference was observed at low-contrast levels ($P_{corrected} = 0.878$), likely due to floor effects.

Interestingly, the results for subjective clarity were slightly different, showing a significant post-cue effect across low, medium, and high contrast levels. Post-hoc comparisons with BONFERRONI correction indicated significant differences between valid and invalid cues across low, medium, and high contrast levels (low: $P_{corrected} = 0.002$; medium: $P_{corrected} < 0.001$; high: $P_{corrected} = 0.021$). This discrepancy is possibly due to floor and ceiling effects.

In the mind-wandering tasks, almost all subjects reported that they were focusing on the Gabor patch in over 70% of the trials, as well as on the dimming of the circle or the fixation cross (Figure 3E, Average = 0.9589, SD = 0.07918). In the speeded-response task, almost all subjects responded accurately and quickly (in less than 1 second) to press the button (Figure 3E, Average = 0.9920, SD = 0.00862).

EEG Results

The P3b in the report and no-report conditions in experiment 3

The P3b analysis results (detailed in the Methods section) are shown in Figure 4A, 4B. In the report condition, significant post-cue P3b effects were observed exclusively at the medium-contrast (75%) level [valid vs. invalid cues: $t(19) = 28.017$, $p < 0.001$; Figure 3.6.1], indicating that post-cue attention enhances visual perception. However, no P3b amplitude differences were found at low- [$t(19) = 0.229$, $p = 0.638$] or high-contrast levels [$t(19) = 0.52$, $p = 0.093$], consistent with prior behavioral findings (10). When comparing P3b amplitudes between high- contrast and low-contrast attentional conditions, we observed a consciousness-related perceptual effect driven by Gabor contrast differences [$t(19) = 28.017$, $p < 0.001$; Figure 4A].

In contrast, under the no-report condition, P3b amplitudes showed no significant differences across all contrast levels [high: $t(19) = 2.516$, $p = 0.129$; medium: $t(19) = 0.344$, $p = 0.565$; low: $t(19) = 0.001$, $p = 0.882$; Figure 4B], nor was there evidence of contrast-driven conscious perception effects [$t(19) = 2.516$, $p = 0.129$; Figure 4B] (13-15).

Notably, when plotting P3b amplitudes across all six conditions (low-invalid, low-valid, medium-invalid, medium-valid, high-invalid, high-valid) in the report task, we observed a nonlinear,

bifurcated growth pattern (16-18). This pattern has been hypothesized as a potential marker of conscious processing. However, despite our linear progression of contrast levels, the attentional modulation (valid/invalid) did not form a linear pattern, precluding further systematic analysis of this phenomenon.

The VAN in the report and no-report conditions in experiment 3

The Visual Awareness Negativity (VAN), defined as a more negative ERP signal for visible versus invisible stimuli (Pitts et al., 2014), exhibits a bilateral posterior distribution primarily within the 150-300 ms time window. VAN analysis results are shown in Figure 4C, 4D. In the report condition, significant post-cue VAN effects were observed exclusively at the high-contrast (100%) level [high: valid vs. invalid, $t(19) = 13.19$, $P = 0.002$; medium: $t(19) = 0.023$, $P = 0.882$; low: $t(19) = 0.164$, $P = 0.690$; Figure 4C]. Notably, the VAN demonstrated an inverse pattern to the P3b, with larger amplitudes under invalid compared to valid cue conditions. When comparing VAN amplitudes between high- contrast and low-contrast attentional conditions, we identified a consciousness-related perceptual effect driven by Gabor contrast differences [$t(19) = 7.33$, $P < 0.001$; Figure 4C]. Mirroring the P3b pattern, no significant VAN differences emerged between valid and invalid trials in the no-report condition [high: $t(19) = 1.251$, $P = 0.277$; medium: $t(19) = 0.023$, $P = 0.882$; low: $t(19) = 0.001$, $P = 0.981$; Figure 4D]. However, high-contrast VAN amplitudes remained significantly larger than low-contrast amplitudes [$t(19) = 3.69$, $P = 0.005$; Figure 4D], indicating preserved contrast-driven conscious perception effects in the no-report condition, consistent with previous studies (15, 19).

Multivariate Analysis Results

We trained linear classifiers for all 62 electrodes to distinguish between target and no-target conditions, using the amplitude across electrodes as features. Classifier performance was evaluated using the area under the curve (AUC) of the receiver operating characteristic (ROC) curve.

Decoding Time Courses in the report condition and no-report condition in experiment 3

However, the temporal profiles of decoding performance varied across different contrast and congruency conditions (Figures 5A, 5B). In the report task, significant clusters emerged earlier after stimulus onset in the valid condition compared to the invalid condition for all three contrast conditions (all $P_{cluster} < 0.05$, shown by different color horizontal bars in Figure 5A top). The temporal profiles of difference AUC (valid-invalid) revealed that significant clusters emerged around 400ms after stimulus onset and ended around 500ms in both high and medium contrast conditions (Figure 5A bottom).

In the no-report task, significant clusters emerged only 300ms after stimulus onset in the high contrast-valid condition, but not in the other five conditions (all $P_{cluster} < 0.05$, shown by different color horizontal bars in Figure 5B top). The temporal profiles of difference AUC (valid-invalid) showed that significant clusters emerged around 400ms and ended around 700ms after stimulus onset in only high contrast conditions (Figure 5B bottom).

Searchlight Decoding Analysis in valid and invalid condition in the Report condition and No-report condition in experiment 3

To identify the regions with the highest decoding performance in valid and invalid conditions across three Gabor contrasts, we conducted a Searchlight Decoding Analysis(20, 21). In the report task, the highest performance cluster was localized to the frontoparietal region electrodes in both medium and high contrast conditions (Supplement Figure 1A). However, in the no-report task, the highest performance cluster emerged in a region much closer to the occipital area, specifically in the high contrast condition (Supplement Figure 1B).

Temporal Generalization Analysis in the Report Condition and No-report Condition in Experiment

These findings demonstrate that the retro-cue effect can improve EEG decoding performance for the target Gabor patch and advance its decoding time, regardless of report or no-report task conditions. To test the temporal generalization performance of the retro-cue effect, we applied the temporal generalization method. In this approach, classifiers are trained on data from each time point separately but tested on all time points, resulting in a temporal generalization matrix (TGM; target present vs. target absent: Supplement Figure 2). Successful decoding between time points

(off-diagonal decoding) indicates that the direction in state space discriminating between target and no-target conditions remains stable over time.
The temporal generalization analysis revealed patterns consistent with the temporal decoding results. In the report task, robust evidence for metastable representations associated with conscious perception was observed across all conditions except the low-contrast-invalid condition (Supplement Figure 2A), manifested as late-stage square patterns in the temporal generalization matrices (16, 18, 22). These late-stage square patterns exhibited greater prominence under valid compared to invalid cue conditions. In contrast, under the no-report condition, such patterns were only detectable in the high-contrast-valid condition (Supplement Figure 2B).
As with the temporal decoding analysis, we created a similar difference-AUC TGM matrix. In the report task, significant clusters emerged around 400ms after stimulus onset and ended around 500ms in both high and medium contrast conditions (Supplement Figure 2A, all $P_{cluster} < 0.05$). In the no-report task, significant clusters emerged around 400ms and ended around 700ms after stimulus onset in only high contrast conditions (Supplement Figure 2B, all $P_{cluster} < 0.05$).
Interestingly, in both analyses, the no-report high contrast condition contributed the longest significant time courses in the difference-AUC analysis, indicating an even longer-lasting retro-cueing perception effect.

Discussion

This study aimed to systematically investigate the relationship between retroactive attention and visual consciousness, focusing on three core questions: 1) distinguishing between sensory-mediated and attention-driven mechanisms underlying retroactive attention effects; 2) determining whether retroactive attention persists under unconscious conditions; and 3) isolating neural activity specific to conscious perception from task-report confounds to confirm whether retroactive cueing genuinely enhances consciousness. To address these questions, we designed three experiments using a paradigm adapted from Sergent et al.(1), requiring participants to report targets (Gabor patches) within 1.5 seconds while eliminating positional uncertainty.

The N2pc is associated with the subliminal retro-cueing effect.

In Experiment 1, we replicated Sergent et al.'s (1) findings under visible cue conditions, observing retroactive attention effects in orientation discrimination tasks at a 66.7 ms stimulus-onset asynchrony (SOA). Critically, these effects persisted even with invisible cues, directly validating our first hypothesis: backward masking does not disrupt sensory-mediated retroactive attention, indicating that bottom-up attentional mechanisms can operate independently of consciousness. This supports the single dissociation hypothesis (attention functions without consciousness) over the interdependence hypothesis (which predicts that retroactive attention effects vanish under unconscious conditions).
Experiment 2 further confirmed these findings via EEG. Analysis of the N2pc component—a classic attention-related ERP—revealed significant differences between valid, no-cue, and invalid conditions. This neural signature indicates unconscious retroactive cues enhance exogenous attention to targets. By modulating masking strength, we dissociated two types of retroactive attention effects, aligning with temporal windows observed in prior work (5).
While earlier studies examined N2pc in unconscious cueing paradigms (23-25), they focused on cue-locked rather than target-locked N2pc. Our Experiment 2 demonstrated target-locked N2pc differences, confirming that unconscious retroactive cues facilitate attentional engagement with targets. This component may serve as a reliable marker for future studies on unconscious spatial retroactive attention.

The controversy on P3b and VAN.

The debate over whether the P3b or visual awareness negativity (VAN) constitutes a neural correlate of consciousness (NCC) remains central to consciousness research (7, 13, 26). Classical report paradigms have long associated P3b with conscious perception (12), but recent no-report studies argue that P3b may instead reflect motor preparation processes tied to task-specific responses, disqualifying it as a pure NCC marker (15). This view was further complicated by(18), who identified a late negative component in the P3b time window during auditory no-report tasks, correlating with graded stimulus intensity. Adding to the complexity, Cohen and

Hense (16, 27) recently proposed N2 as a potential consciousness marker, reigniting debates about the temporal and functional specificity of NCC candidates.
Our findings challenge the outright dismissal of P3b's role in consciousness. Under no-report conditions, we observed attenuated but persistent P3b activity (300–600 ms) for high-contrast stimuli, though differences between contrast levels were statistically nonsignificant (Figure 4B). Critically, multivariate pattern analysis (MVPA) revealed stable late-stage conscious representations (>300 ms) specifically in high-contrast valid trials, suggesting that late potential like P3b may still index aspects of conscious processing even when explicit reporting is absent. These results question the prevailing assumption that P3b solely reflects post-perceptual motor preparation (15), instead implicating it in the maintenance or amplification of conscious content.
However, our conclusions face potential critiques:
Covert Reporting Strategies: The inclusion of complex tasks (e.g., color discrimination, mind-wandering checks) might inadvertently encourage participants to adopt internal reporting strategies, reintroducing task-related confounds (28).
Motor Preparation Contamination: Frequent keypress requirements (e.g., rapid responses) could amplify motor-related potentials, masking genuine NCC signals.
To address these concerns, we implemented rigorous controls: Mitigating Covert Strategies: Half of the participants performed the no-report task before the report task, ensuring no prior knowledge of reporting demands. Subgroup analyses confirmed no behavioral or neural differences between these participants and the full cohort. Isolating NCC Activity: ERP amplitudes were derived by subtracting the blank-cue condition from the target-cue condition, effectively canceling out motor preparation artifacts. Crucially, P3b emerged exclusively in high-contrast valid trials, aligning with NCC characteristics such as stimulus-intensity-dependent bifurcation patterns (18) and temporally stable decoding (16).
These findings underscore methodological limitations in prior no-report studies: Inattentional Blindness: Without eye-tracking validation (19, 29), participants' "satisfactory performance" might reflect inattentional blindness (30) rather than genuine conscious perception. Eye-Movement Fallacy: Extrapolating eye-movement metrics (e.g., pupil responses) from report to no-report conditions is problematic, as eye movements poorly correlate with conscious content (31, 32).
Our results advocate for a nuanced interpretation: while P3b may not fully satisfy NCC criteria, its persistence under no-report conditions—coupled with late-stage MVPA decoding—suggests it plays a transitional role in stabilizing conscious representations. This aligns with (26) the distinction between phenomenal consciousness (VAN-like local activity) and access consciousness (P3b-related global broadcasting), proposing that P3b bridges sensory processing and conscious access.
Ultimately, the P3b/VAN debate reflects deeper tensions in defining consciousness itself. Is consciousness a discrete neural event or a dynamic process spanning multiple stages? Our data favor the latter, emphasizing the need for experimental designs that disentangle attention, perception, and reporting while rigorously validating conscious states—a challenge that remains central to future NCC research.

Retrospective attention as a trigger for conscious perception

To rigorously test whether retroactive attention directly enhances conscious perception across varying stimulus intensities (1, 2), experiment 3 employed a no-report paradigm. A critical prediction was formulated: If neural signatures (e.g., ERP amplitudes, decoding performance) showed no difference between valid and invalid retro-cue conditions in the absence of reporting, retroactive attention would merely amplify attentional prioritization. Conversely, enhanced ERP components linked to consciousness or improved/earlier neural decoding of target Gabors would confirm that retroactive attention boosts conscious perception itself.
This experimental design directly addresses the second hypothesis proposed in our introduction: that retroactive attention persists and enhances conscious perception even in a no-report paradigm. According to the prediction of the single dissociation hypothesis, we should observe that retroactive attention enhances conscious perception even after excluding the influence of task-related cognitive processes.

The present results replicate previous findings on the retroactive effects of attention on conscious perception (1, 2). Notably, the subjective visibility results demonstrated significant post-cue effects across low, medium, and high contrast levels, a finding not paralleled by accuracy measurements in the orientation discrimination task. This discrepancy could be attributed to the heightened sensitivity of subjective measures compared to objective measures, which may be susceptible to ceiling and floor effects. While prior studies primarily employed behavioral experiments to verify effects on conscious perception, this study rigorously tested these effects at the neural level through multivariate pattern analysis.

Multivariate pattern analysis, particularly temporal generalization analysis, has mainly been applied in conscious perception experiments involving linearly increasing physical intensities (1, 16, 22, 33). However, Mathieu Landry and colleagues (34) recently used this method to distinguish between the neural signatures of exogenous and endogenous spatial cueing attention. Their study elegantly demonstrated how multivariate pattern analysis could corroborate earlier observations from behavioral and ERP measures. In the present study, we adopted a similar strategy to investigate the effects of retroactive attention at the neural level. A comparison of 12 different conditions confirmed that retro-cued attention indeed improves the conscious perception of Gabor patches. The decoding performance revealed a distinct pattern, showing that the benefits of retro-cued attention stem from the enhancement of neural signatures of consciousness during later time courses (400–700 ms), consistent with previous studies (Figure 5, 6A) (1, 16, 33).

These findings dismiss the hypothesis that the retroactive attention effect arises from working memory rather than perceptual processing. If retro-perception merely prevented the rapid decay of representations stored in working memory, we would have observed no significant differences in neural signals between valid retro-cue trials and invalid or no-cue trials in the no-report task, as this design excluded task-related processes and required no stimulus memorization. However, the data showed clear evidence of neural signal enhancement. Contrary to the widely held assumption that events occurring after stimulus disappearance affect only post-perceptual processes, such as decision-making or working memory (35-37), our results demonstrate that retro-cued attention can directly influence whether a stimulus is consciously perceived at the neural level. This aligns with a recent study on retroactive perception using a mixed-model analysis approach (2).

The relationship between attention and consciousness

Contemporary theories on the relationship between attention and consciousness propose three main perspectives: the dual dissociation of attention and consciousness (9), single dissociation (10), and no dissociation (11). In the introduction, we proposed three hypotheses to systematically test three different theories on the relationship between attention and consciousness: Backward masking paradigms do not interfere with sensory-mediated retroactive attention effects; retroactive attention persists and enhances conscious perception in no-report paradigms. These findings will systematically support the single dissociation hypothesis.

Our data support the single dissociation view between attention and consciousness. In Experiments 1 and 2, we demonstrated that retroactive attention modulates perceptual processing under unconscious conditions. Furthermore, in Experiment 3, retroactive attention enhanced conscious perception even in a no-report paradigm under high-contrast conditions, indicating that attention continues to play a role in conscious perception after controlling for decision- and motor-related neural activity.

Specifically, using a retro-cued spatial attention paradigm (1), our results show that spatial attention can modulate consciousness 67 ms after target presentation under purely perceptual conditions. This reveals a highly flexible temporal window for attentional modulation of consciousness, providing compelling experimental evidence for the single dissociation hypothesis and validating Hypothesis 3.

Our findings challenge the dual dissociation hypothesis. If attention and consciousness were fully separable, we should have observed retroactive attention affecting only attention-related neural markers (e.g., N2pc) without influencing neural correlates of conscious perception. However, our ERP and multivariate pattern analyses revealed that retroactive attention not only enhanced

attention-related components like the N2pc but also directly amplified consciousness-related neural representations, demonstrating that attention directly shapes conscious perception itself. Similarly, our results contradict the no-dissociation hypothesis. If attention and consciousness were identical, no retroactive attention effects should have been observed under unconscious conditions. Yet, Study 1 demonstrated that retroactive attention remained functional even when cues were invisible, indicating that attention can operate independently of consciousness.

Searchlight and neural correlates of consciousness

The Searchlight Decoding Analysis in Experiment 3 revealed distinct neural patterns associated with the Report and No-report conditions under valid and invalid scenarios across varying Gabor contrasts. In the Report condition, the highest decoding performance clusters were consistently localized within the fronto-parietal regions, particularly under medium and high contrast conditions (Figure 6B; Supplement Figure 1A). This localization suggests that the frontoparietal network, known for its role in attention and decision-making processes, is actively engaged when participants are required to report their perceptions, especially when the visual stimuli are more salient. In contrast, the No-report condition demonstrated peak decoding performance near the occipital areas, notably under high contrast conditions (Figure 6B; Supplement Figure 1B). This parieto-occipital dominance aligns with the primary visual processing functions of the occipital lobe, indicating that in the absence of a reporting task, neural activity remains more confined to sensory processing regions, consistent with previous research on consciousness (14, 15, 19, 29). The shift from frontoparietal to occipital regions between Report and No-report conditions highlights the modulatory effect of task demands on neural engagement. Specifically, the requirement to report appears to recruit higher-order cognitive networks beyond primary sensory areas, whereas the No-report condition allows for more localized sensory processing. These findings underscore the dynamic interplay between attention, perception, and executive functions and suggest that task instructions can significantly influence the spatial distribution of neural decoding performance.

Although late components in ERP, time decoding, and time generalization analyses are capable of decoding attention and consciousness, our Searchlight Decoding Analysis within the late time window (400 ms–600 ms) still indicates that, under no-report conditions, the decoding locations for attention and consciousness remain near posterior brain regions rather than encompassing the whole brain or the prefrontal cortex. However, due to the low spatial resolution of EEG, we are unable to localize the cortical sources of these decoding signals. Therefore, these findings warrant further investigation using higher spatial resolution techniques, such as fMRI and iEEG.

Limitations of the study

It is noteworthy that in the no-report task, we only observed the retrospective attention effect in the high-contrast condition. This may be due to our use of an adapted Posner Cueing Paradigm(38), which is typically employed in spatial attention research rather than studies on consciousness. As a result, participants were required to divide their attention between two locations simultaneously. In the no-report task, however, participants were asked to perform a task entirely unrelated to the stimulus, thus allocating less attention to the target stimulus. Consequently, the contrast threshold for the Gabor patches may have increased. This is evident in the medium contrast condition, where the decoding performance in the invalid condition was higher than in the valid condition (Figure 5B, 6B) when attention was not fully focused on the Gabor task. In other words, the cue presented at the same location produced an interference effect—similar to a backward masking effect (12, 39).

Previous studies on the bifurcation model of consciousness have generally employed stimuli with the same physical intensity in both report and no-report tasks (16, 18, 40), and this study followed that approach as well. In the field of consciousness research, some researchers have used eye-movement measurements to ensure that physical stimuli are visible even when participants do not provide explicit reports (28, 32, 41). Therefore, in future studies on the retrospective spatial cueing effect, it would be advisable to include eye movement measurements to ensure that participants' subjective visibility in no-report tasks does not significantly differ from their visibility in report tasks.

Additionally, although we controlled for the sequence effects of the report and no-report tasks (see Methods), we did not specifically examine the potential impact of the order of these sessions, which has been rigorously tested in a previous study (18). Lastly, we did not investigate potential sex/gender differences in retrospective attention effects, which could be a valuable avenue for future research.

Future Directions and Practical Implications

Based on our findings, future studies should explore integrating eye-tracking measurements with retro-cue paradigms to better delineate the relationship between attention and conscious perception. This will help further validate the theoretical hypotheses on the attention-consciousness relationship proposed in the Introduction, particularly in distinguishing P-consciousness from A-consciousness (26), as well as conscious content from conscious states. Additionally, future research could investigate how different types of attention (e.g., feature-based attention, object-based attention, top-down attention) influence retro-perception (42-45). This would advance a comprehensive understanding of the mechanisms through which attention shapes consciousness and enrich the attentional taxonomy framework discussed in the Introduction. Exploring gender differences may also provide deeper insights into the universality of retroactive attention effects. Expanding the scope of task complexity and stimulus categories could further clarify the boundaries of retroactive attention effects.

From a practical perspective, our findings hold potential applications in attention-training programs and cognitive rehabilitation therapies. Enhancing conscious perception through retroactive attention might aid the recovery of individuals with attention deficits or impaired cognitive functions. Furthermore, understanding the neural mechanisms of attention and consciousness could guide the development of neurofeedback and brain-computer interface technologies to optimize cognitive performance (46).

In summary, through three meticulously designed experiments, this study systematically validated the effects of retroactive attention on conscious perception and provided robust support for the single dissociation hypothesis regarding the attention-consciousness relationship. Our findings demonstrate that attention can operate independently under unconscious conditions, yet the formation of consciousness relies on the engagement of attentional resources. This conclusion not only enriches our understanding of attention and consciousness—two core issues in cognitive neuroscience—but also offers new directions and methodological insights for future research.

Materials and Methods

Experimental Model and Study Participant Details

A total of 29 human subjects (9 male, 18–28 years old) were involved in Experiment 1, Standard Deviation = 2.94. Twenty-four of them participated in Experiment 1, and 5 participants (4 males, 1 female) were excluded from analysis due to excessively high or low overall behavioral accuracy (below 65% or above 85%) in the formal experiment, which invalidated the threshold test. After exclusion, the gender ratio became male-to-female = 5:19. 23 human subjects (9 male, 18–29 years old) participated in Experiment 2, but one subject (female) in Experiment 2 was excluded because of too many artifacts (>10% trials were discarded). 20 human subjects (9 male, 18–29 years old) participated in Experiment 3, and no subject was excluded. The sample size was based on the previous study regarding retro-cueing attention and a priori power calculation using the G*Power program (47). The power analysis indicated that a sample of 24, 23, and 20 in our behavioral and EEG experiments, respectively, would be sufficient to detect a medium-size effect ($f = 0.35$) in a within-subjects analysis of ANOVA with a power of 0.8. They were naive to the purpose of the study, except for one subject in Experiment 3 (One of the authors). They were right-handed, reported normal or corrected-to-normal vision, and had no known neurological or visual disorders. They gave written informed consent, and our procedures and protocols were approved by the human subjects review committee of the School of Psychology at South China Normal University.

METHOD DETAILS

Stimuli

In both Experiment 1 and Experiment 2, the stimuli consisted of two horizontally arranged black circles (1.3 cd/m², 3° visual angle in diameter) on the screen, along with a central fixation cross

(1.3 cd/m², 0.5° visual angle) for fixation. These circles were positioned 5° to the left and right of the fixation point. The experimental procedure was divided into a threshold-testing phase and a formal experiment phase. Cues were briefly presented (16.67 ms) as a dimming (20 cd/m²) of one of the two black circles, followed by a longer dimming (83.33 ms) of both circles (with brightness adjusted for each participant) to mask the cue in the Invisible Cue conditions. In the Visible Cue conditions, there was no dimming, and a fixation screen was shown instead. The target stimulus was a Gabor patch (2° visual angle in diameter) tilted either 30° or 150° from the vertical. In Experiment 3, the stimuli were similar to those in Experiment 1 and Experiment 2, with the following adjustments: the diameter of the black circles was increased to a 4° visual angle, and the diameter of the Gabor patch was increased to a 3° visual angle. Additionally, the two black circles were positioned 5° above and below the fixation point rather than to the sides.

Behavioral experiments Overview

The experiment was programmed using Psychtoolbox based on Matlab2016b (48). All stimuli were presented on a 19-inch LED computer screen with a resolution of 1024×768 and a refresh rate of 60 Hz. The background was gray (28 cd/m²).

In Experiment 1, two horizontally arranged black circles (1.3 cd/m², 3° visual angle in diameter) were always present on the screen. In Experiment 2, the black circles on the left and right sides were shifted downward by 2.5° of a visual angle compared to Experiment 1. In Experiment 3, two vertically arranged black circles (1.3 cd/m², 4° visual angle in diameter) were used instead. A fixation cross (1.3 cd/m², 0.5° visual angle) was used for fixation.

In Experiment 1 and Experiment 2, the black circles were positioned 5° to the left and right of the fixation point. In Experiment 3, the black circles were positioned 5° above and below the fixation point. The viewing distance was 57 cm, and participants' head positions were stabilized using a chin rest. The black fixation cross was always displayed at the center of the screen.

Threshold measurement task

Before each Retro-Cueing Spatial Attention (RCSA) task, participants first performed a two-alternative forced-choice (2AFC) judgment to determine the location of the cue stimulus—either to the left or right of the fixation point in Experiment 1 and Experiment 2, or above or below in Experiment 3. Accuracy in the visible cue condition was maintained above 95%, while in the invisible cue condition, it was kept at 50%, i.e., chance level. Following this, we measured the orientation discrimination thresholds of the target Gabor using a 2AFC staircase procedure aimed at achieving 75% accuracy. This was done to ensure equal performance across both visible and invisible cue conditions. The stimuli and procedure for this threshold measurement task were identical to those of the RCSA task, except that no cue stimuli were presented. The contrast discrimination threshold measurement task consisted of two sessions: one for the visible condition (without a Mask stimulus) and one for the invisible condition (with a Mask stimulus). The order of these sessions was counterbalanced across participants. Each session included two staircases of 80 trials each. Each trial began with a central fixation point. Participants were instructed to press one of two buttons to indicate the orientation of the target Gabor. The contrast of the target Gabor varied from trial to trial and was controlled by the staircase procedure to estimate the participants' orientation discrimination threshold at a 75% correct level.

Experiment1

Each participant completed four staircase sessions (80 trials each): two for the visible cue condition and two for the invisible cue condition. These sessions determined the target's contrast at which participants could discriminate the target's orientation with 75% accuracy, without any attentional manipulation. This contrast value was then fixed for the remainder of the experiment. Participants subsequently performed four experimental blocks, each consisting of 288 trials, resulting in 96 trials for each combination of cueing and SOA conditions.

As shown in Figure 1A, each trial commenced with the appearance of a fixation cross at the center. After a random delay of 800 to 1200 ms, a target—a Gabor patch with a random orientation (30° or 150° away from the vertical)—was displayed for 33.33 ms within one of the circles located to the left or right of the fixation point. The target contrast was individually calibrated for each participant using a staircase method. A 16.67 ms cue, consisting of a brief dimming of one of the circles, could appear either before or after the target. This cue could be

either valid (on the same side as the target) or invalid (on the opposite side). Following the cue, there was an 83.33 ms mask or fixation period for the invisible and visible conditions.
A response screen was presented 800 to 1200 ms after the offset of the mask or fixation, with a response cue indicating the target's side (marked by thickening and dimming on one side of the cross). Participants were then asked to report the target's orientation by choosing between two options (Left/Right). Subsequently, a second response screen appeared, displaying a dimming cross at the fixation point, where participants reported the position of the cue in a two-alternative forced choice (2AFC) task.

Experiment2

Each participant completed two staircase sessions (80 trials each) for the invisible cue condition to determine the target's contrast at which they could discriminate the target's orientation with 75% accuracy, without any attentional manipulation. This contrast value was then fixed for the remainder of the experiment. Participants subsequently performed four experimental blocks, each consisting of 153 trials, resulting in 136 trials for each cueing condition, including the non-cue condition and catch trials (33.33%).
The stimulus presentation for the EEG experiment was consistent with that of Experiment 1. The procedure in Experiment 2 was fundamentally similar to Experiment 1, with the following modifications: the two circles were placed below the fixation point (shifted downward by 2.5° of a visual angle compared to Experiment 1); the target presentation screen included a fixation screen with a 33.33% probability (catch trials); the stimulus onset asynchrony (SOA) between the target and the cue was fixed at 66.67 ms; a Non-Cue condition was added to the cue presentation; and only the mask stimulus was presented, thereby maintaining only the invisible condition.

Experiment3

Each participant completed six staircase sessions (80 trials each) for the visible cue condition to determine the target's contrast at which they could discriminate the target's orientation with 50%, 75%, and 100% accuracy, without any attentional manipulation. These determined contrast values were then fixed for the remainder of the experiment. Participants subsequently performed four experimental blocks, each consisting of 196 trials, resulting in 112 trials for each cueing condition, including the catch trials (25%).
As shown in Figure 1C, in this experiment, two circles were positioned above and below the fixation point. The Gabor patch and the cue randomly appeared in one of the two circles. The physical stimulus intensity was determined for each participant based on the Gabor contrast levels obtained from the staircase test: high contrast for near 100% orientation discrimination accuracy, medium contrast for approximately 75% accuracy, and low contrast for about 50% accuracy. The fixation screen from Experiment 2 was retained for catch trials.
As shown in Figure 1D, on the response screen, the active reporting condition remained similar to the Gabor patch orientation discrimination task from the previous experiment. However, participants were now required to identify both the orientation of the Gabor patch (Left or Right) and rate the subjective visibility ("visible" or "invisible") simultaneously. Thus, in each trial, participants had four response options.
Additionally, a passive viewing condition was introduced, wherein participants were required to complete one of three randomly presented tasks:
1. Speed Response Task: Press the SPACE key whenever a green cross was displayed at fixation.
2. Mind-Wandering Detection Task: Participants answered the question "What is on your mind just now?" by choosing one of four options: "the Gabor/Fixation," "the cross," "my thoughts," or "nothing/I feel sleepy."
3. A Simple Message Prompt: "Press SPACE to continue."

EEG data Acquisition

Sixty-four electrodes were placed according to the international 10-20 system to collect EEG data, using the Brain Products EEG amplifier (Brain Products, Munich, Germany) for signal amplification. During recording, the impedance of all electrodes was kept below 10 kΩ. The frontal electrode FCz served as the online reference point, while the electrode AFz served as the ground. No online filtering was applied to the electrodes, and continuous sampling was performed

at a frequency of 1000 Hz per channel. Eye movements and blinks were monitored using the IO channel located under the right eye.

Data Preprocessing

Offline preprocessing of EEG data was performed using BrainVision Analyzer 2.2 (Brain Products) and the EEGLAB toolbox (49). Firstly, visual identification of any noisy electrodes was performed, and interpolation of surrounding electrodes was used to reconstruct the noisy channels if necessary. All electrodes were then re-referenced to the average of the left and right mastoids. Then, all EEG signals underwent a series of filters: 0.1 Hz high-pass, 25 Hz low-pass, and 50 Hz notch filtering with a 24 dB/Oct roll-off. Vertical eye blink correction and horizontal eye drift correction were also applied. Segmentation of trials around the target (or the same time point in cue-mask-only trials). Segments containing peak-to-peak deviations exceeding ±70 μV were excluded from the analysis, and if the number of excluded segments exceeded 20% of the total trials, the data from that participant were discarded. Baseline correction using the time window from -100 to 0ms pre-stimulus.

ERPs and cue, cue-mask subtraction

Trials were sorted by condition and trial type (valid, invalid, or cue/cue-mask only). Each group of trials was averaged at the participant level and low-pass filtered at 25 Hz. To isolate stimulus-related neural activity from cue/cue-mask-evoked activity, the cue/cue-mask-only ERPs were time-shifted to align the timing of the cues with cue onset in the stimulus-cue-mask trials, following the procedure of Del Cul and Cohen (12, 16). This was done for each condition, and the time-shifted mask ERPs were subtracted from the corresponding stimulus-cue-mask ERPs as follows:

The cue/cue-mask-only ERP is initially time-locked to cue onset (i.e., time 0 is when the first cue was presented).

The cue/cue-mask-only ERP is then shifted forward in time so that cue onset aligns with cue onset in each of the stimulus-cue-mask ERPs.

The time-shifted mask ERPs are subtracted from the corresponding stimulus-cue-mask ERPs.

ERP analysis

Three ERPs of interest were identified based on data from the initial group: the N2pc in Experiment 2, the VAN in Experiment 3 (both displaying bifurcation dynamics in the no-report condition), and the P3b (displaying bifurcation dynamics in the report condition). The following time windows and electrodes were selected for each component (nearest channels of the international 10-20 system are reported in parentheses):

N2pc: 240-280 ms, electrodes (O1/O2, PO3/PO4, PO7/PO8).

P3b: 300-600 ms, electrodes (Pz, P1, P2, CPz, CP1, CP2, Cz).

VAN: 240-280 ms, electrodes (P5, P6, P7, P8, PO7, PO8).

These time windows and electrodes were used for all analyses of these three ERPs. Additionally, a post-hoc analysis of the VAN was conducted, measured from 240-280 ms at electrodes (P5, P6, P7, P8, PO7, PO8).

Multivariate pattern analysis

All decoding was conducted using the MVPA-Light toolbox and fieldtrip for MATLAB (21, 50). Data was exported from BrainVision Analyzer and formatted for use with the MVPA-Light toolbox using EEGLAB. For each cue validity and task condition, a linear classifier (LDA) was trained to distinguish between stimulus-present and cue-mask-only trials using a 9-fold cross-validation procedure.

At each time point, the decoder was first trained on 8/9 of the trials and then tested on the remaining subset of trials. This process was repeated nine times, ensuring that the decoder was both trained and tested on the entire dataset over the course of the procedure. Importantly, the classifier was never tested on data used for training when assessing performance.

Trial numbers were balanced across classes so that there were equal numbers of stimulus-present and cue-mask-only trials in each fold. Classifier sensitivity, summarized as the area under the receiver operating characteristic curve (AUC), was averaged across the folds to calculate overall classifier performance.

Temporal generalization analysis

The temporal generalization analysis technique characterizes the neural dynamics of perceptual representations by testing if a classifier trained on data from one time point can successfully discriminate between classes when applied to data from different time points. If a classifier trained at time T1 can decode stimulus presence at a level significantly above chance when tested at time T2, it suggests that the neural dynamics supporting above-chance decoding at T1 are recurring at T2.

Temporal generalization matrices were computed by training classifiers on one time point and testing each at every other time point. Classification sensitivity was statistically tested against chance and corrected for multiple comparisons using 1000-permutation cluster-based permutation testing.

Searchlight analysis

To identify the electrodes that made the most significant contributions to decoding performance across temporal bins, we employed searchlight analysis. In this approach, time served as the feature matrix, allowing us to quantify the decoding performance of each electrode neighborhood. The procedure began by calculating the square distance between electrodes based on their X and Y coordinate positions. Subsequently, we applied specific temporal windows—400-500 ms for the report condition and 400-600 ms for the no-report condition—and conducted classification at each corresponding window. Decoding performance was computed using the MVPA-light package with Linear Discriminant Analysis (LDA) as the classifier, implementing a 9-fold stratified cross-validation methodology (21). We maintained methodological consistency by applying an equivalent trial matching procedure across all 12 experimental conditions.

Acknowledgments

We acknowledge the subjects for their contribution to this study. This work was supported by National Outstanding Youth Science Fund Project of National Natural Science Foundation of China (32022032), and National Natural Science Foundation of China General Program (32271099).

Data Availability

The anonymized datasets for this study are available at Open Science Framework, https://osf.io/mjqwb/.

References

1. C. Sergent *et al.*, Cueing attention after the stimulus is gone can retrospectively trigger conscious perception. *Curr Biol* **23**, 150-155 (2013).
2. L. Thibault, R. van den Berg, P. Cavanagh, C. Sergent, Retrospective Attention Gates Discrete Conscious Access to Past Sensory Stimuli. *PLoS One* **11**, e0148504 (2016).
3. S. Dehaene, J.-P. Changeux, L. Naccache, J. Sackur, C. Sergent, Conscious, preconscious, and subliminal processing: a testable taxonomy. *Trends in cognitive sciences* **10**, 204-211 (2006).
4. V. A. Lamme, Why visual attention and awareness are different. *Trends in cognitive sciences* **7**, 12-18 (2003).
5. Y. Xia, Y. Morimoto, Y. Noguchi, Retrospective triggering of conscious perception by an interstimulus interaction. *J Vis* **16**, 3 (2016).
6. S. Dehaene, H. Lau, S. Kouider, What is consciousness, and could machines have it? *Science* **358**, 486-492 (2017).
7. J. Aru, T. Bachmann, W. Singer, L. Melloni, Distilling the neural correlates of consciousness. *Neuroscience and biobehavioral reviews* **36**, 737-746 (2012).
8. P. M. Bays, R. Taylor, A neural model of retrospective attention in visual working memory. *Cognitive Psychology* **100**, 43-52 (2018).
9. C. Koch, N. Tsuchiya, Attention and consciousness: two distinct brain processes. *Trends in Cognitive Sciences* **11**, 16-22 (2007).
10. S. Dehaene, J. P. Changeux, Experimental and theoretical approaches to conscious processing. *Neuron* **70**, 200-227 (2011).

11. V. Wyart, S. Dehaene, C. Tallon-Baudry, Early dissociation between neural signatures of endogenous spatial attention and perceptual awareness during visual masking. *Frontiers in human neuroscience* **6**, 16 (2012).
12. A. Del Cul, S. Baillet, S. Dehaene, Brain Dynamics Underlying the Nonlinear Threshold for Access to Consciousness. *PLOS Biology* **5**, e260 (2007).
13. N. Tsuchiya, M. Wilke, S. Frässle, V. A. F. Lamme, No-Report Paradigms: Extracting the True Neural Correlates of Consciousness. *Trends in Cognitive Sciences* **19**, 757-770 (2015).
14. T. Dellert *et al.*, Dissociating the Neural Correlates of Consciousness and Task Relevance in Face Perception Using Simultaneous EEG-fMRI. *J Neurosci* **41**, 7864-7875 (2021).
15. M. A. Pitts, J. Padwal, D. Fennelly, A. Martinez, S. A. Hillyard, Gamma band activity and the P3 reflect post-perceptual processes, not visual awareness. *Neuroimage* **101**, 337-350 (2014).
16. M. A. Cohen, C. Dembski, K. Ortego, C. Steinhibler, M. Pitts, Neural signatures of visual awareness independent of postperceptual processing. *Cerebral Cortex* **34** (2024).
17. S. Kouider *et al.*, A Neural Marker of Perceptual Consciousness in Infants. *Science* **340**, 376-380 (2013).
18. C. Sergent *et al.*, Bifurcation in brain dynamics reveals a signature of conscious processing independent of report. *Nat Commun* **12**, 1149 (2021).
19. M. A. Cohen, K. Ortego, A. Kyroudis, M. Pitts, Distinguishing the Neural Correlates of Perceptual Awareness and Postperceptual Processing. *The Journal of Neuroscience* **40**, 4925-4935 (2020).
20. J. A. Etzel, J. M. Zacks, T. S. Braver, Searchlight analysis: promise, pitfalls, and potential. *Neuroimage* **78**, 261-269 (2013).
21. M. S. Treder, MVPA-Light: A Classification and Regression Toolbox for Multi-Dimensional Data. *Frontiers in Neuroscience* **14** (2020).
22. J. R. King, S. Dehaene, Characterizing the dynamics of mental representations: the temporal generalization method. *Trends in Cognitive Sciences* **18**, 203-210 (2014).
23. C. M. Giattino, Z. M. Alam, M. G. Woldorff, Neural processes underlying the orienting of attention without awareness. *Cortex* **102**, 14-25 (2018).
24. M. Mulckhuyse, J. Theeuwes, Unconscious attentional orienting to exogenous cues: A review of the literature. *Acta Psychol (Amst)* **134**, 299-309 (2010).
25. S. Prasad, R. K. Mishra, The Nature of Unconscious Attention to Subliminal Cues. *Vision (Basel)* **3** (2019).
26. N. Block, Two neural correlates of consciousness. *Trends Cogn Sci* **9**, 46-52 (2005).
27. A. Hense, A. Peters, M. Bruchmann, T. Dellert, T. Straube, Electrophysiological correlates of sustained conscious perception. *Sci Rep* **14**, 10593 (2024).
28. S. I. Kronemer *et al.*, Human visual consciousness involves large scale cortical and subcortical networks independent of task report and eye movement activity. *Nat Commun* **13**, 7342 (2022).
29. E. Hatamimajoumerd, N. A. Ratan Murty, M. Pitts, M. A. Cohen, Decoding perceptual awareness across the brain with a no-report fMRI masking paradigm. *Curr Biol* **32**, 4139-4149 e4134 (2022).
30. A. Mack, Inattentional blindness: Looking without seeing. *Current directions in psychological science* **12**, 180-184 (2003).
31. B. J. He, Next frontiers in consciousness research. *Neuron* **111**, 3150-3153 (2023).
32. M. Spering, M. Carrasco, Acting without seeing: eye movements reveal visual processing without awareness. *Trends in Neurosciences* **38**, 247-258 (2015).
33. O. Ferrante *et al.*, An adversarial collaboration to critically evaluate theories of consciousness. *bioRxiv* 10.1101/2023.06.23.546249, 2023.2006.2023.546249 (2023).
34. M. Landry, J. da Silva Castanheira, K. Jerbi, Differential and Overlapping Effects between Exogenous and Endogenous Attention Shape Perceptual Facilitation during Visual Processing. *J Cogn Neurosci* **35**, 1279-1300 (2023).

35. R. A. Kinchla, Z. Chen, D. Evert, Precue effects in visual search: data or resource limited? *Percept Psychophys* **57**, 441-450 (1995).
36. W. Prinzmetal, V. Long, J. Leonhardt, Involuntary attention and brightness contrast. *Perception & Psychophysics* **70**, 1139-1150 (2008).
37. E. K. Vogel, G. F. Woodman, S. J. Luck, Pushing around the locus of selection: evidence for the flexible-selection hypothesis. *J Cogn Neurosci* **17**, 1907-1922 (2005).
38. M. I. Posner, Orienting of attention. *Q J Exp Psychol* **32**, 3-25 (1980).
39. S. Dehaene *et al.*, Cerebral mechanisms of word masking and unconscious repetition priming. *Nat Neurosci* **4**, 752-758 (2001).
40. B. van Vugt *et al.*, The threshold for conscious report: Signal loss and response bias in visual and frontal cortex. *Science* **360**, 537-542 (2018).
41. V. Kapoor *et al.*, Decoding internally generated transitions of conscious contents in the prefrontal cortex without subjective reports. *Nature Communications* **13** (2022).
42. M. Carrasco, Visual attention: the past 25 years. *Vision Res* **51**, 1484-1525 (2011).
43. B. J. Scholl, Objects and attention: The state of the art. *Cognition* **80**, 1-46 (2001).
44. S. Treue, J. C. Martínez Trujillo, Feature-based attention influences motion processing gain in macaque visual cortex. *Nature* **399**, 575-579 (1999).
45. M. Corbetta, G. L. Shulman, Control of goal-directed and stimulus-driven attention in the brain. *Nature Reviews Neuroscience* **3**, 201-215 (2002).
46. J. Bagdasaryan, V. Quyen Mle, Experiencing your brain: neurofeedback as a new bridge between neuroscience and phenomenology. *Front Hum Neurosci* **7**, 680 (2013).
47. F. Faul, E. Erdfelder, A. Buchner, A.-G. Lang, Statistical power analyses using G*Power 3.1: Tests for correlation and regression analyses. *Behavior Research Methods* **41**, 1149-1160 (2009).
48. M. Kleiner, D. Brainard, D. Pelli, What's new in Psychtoolbox-3? (2007).
49. A. Delorme, S. Makeig, EEGLAB: an open source toolbox for analysis of single-trial EEG dynamics including independent component analysis. *J Neurosci Methods* **134**, 9-21 (2004).
50. R. Oostenveld, P. Fries, E. Maris, J.-M. Schoffelen, FieldTrip: Open Source Software for Advanced Analysis of MEG, EEG, and Invasive Electrophysiological Data. *Computational Intelligence and Neuroscience* **2011**, 156869 (2011).

Figures and Tables

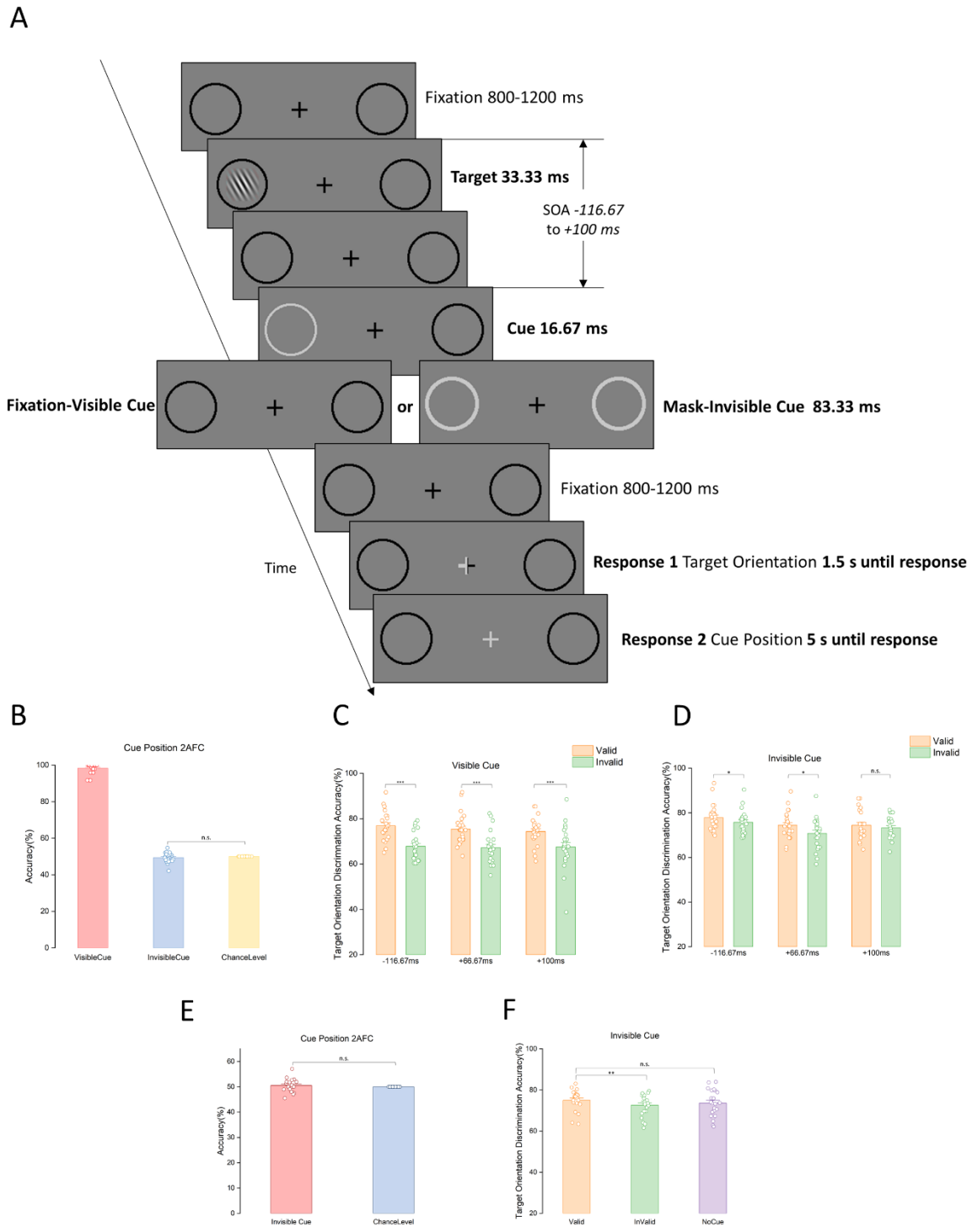

Figure 1. Experiment 1&2 Behavioral Results

(A) In Experiment 1, trials began with a central fixation cross. After 800-1200 ms, a Gabor patch (33.33 ms duration, 30° or 150° orientation) appeared in either the left/right peripheral circle, with contrast individually adjusted via staircase calibration. A 16.67 ms cue (circle dimming) appeared either pre- or post-target, being valid (target side) or invalid (opposite side). An 83.33 ms mask/fixation period followed (visible/invisible conditions). After 800-1200 ms, participants first reported target orientation (left/right binary choice) via a response screen with side-indicator cues, then completed a 2AFC task on a second screen to identify cue location using a dimmed fixation cross.
(B,E) Cue Position Discrimination 2AFC Task in Experiment 1 and 2: Dots represent individual performance. Accuracy is presented on the y-axis, and the different visible cues are presented on the x-axis. Error bars represent the standard error of the mean.
(C,D,F) Target Orientation Discrimination 2AFC Task in Experiment 1 and 2: Dots represent individual performance, with chance level at 50%. Accuracy is presented on the y-axis. The different target-cue SOA conditions are presented on the x-axis. Under the visible cue condition, all three selected target-cue SOA conditions exhibited the classic pre-cue and post-cue effects, with accuracy in the valid cue condition significantly higher than in the invalid cue condition. The middle shows the visible cue condition, while the right shows the invisible cue condition.

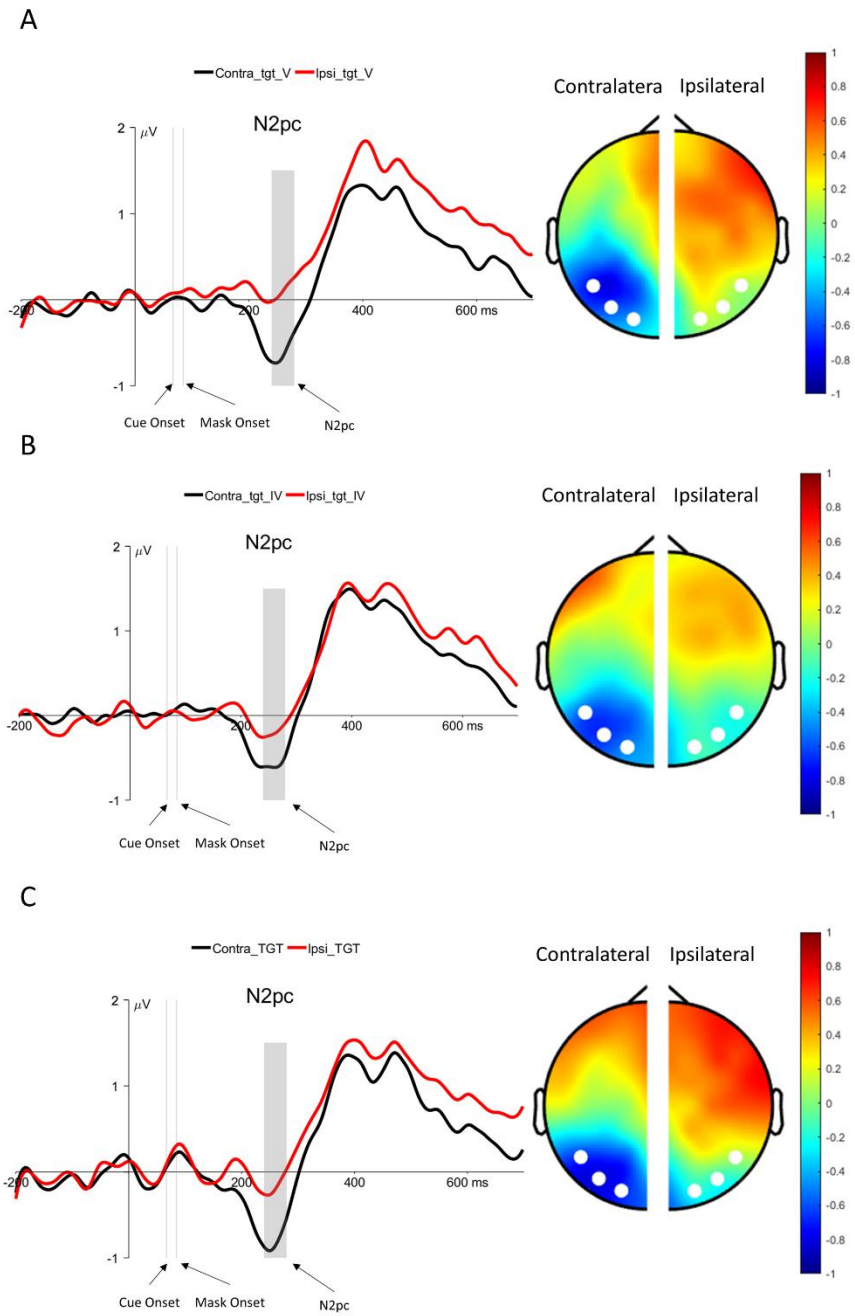

Figure 2. Experiment 2 ERP Results

A-valid, B-invalid, B-non-cue, left: N2pc waveforms for contralateral and ipsilateral sides plotted over time. Shaded areas represent the time window for mean amplitude used for statistical testing (240-280 ms). Right: Topographical voltage distributions between 240-280 ms with all electrodes used to analyze the N2pc indicated on the scalp map.

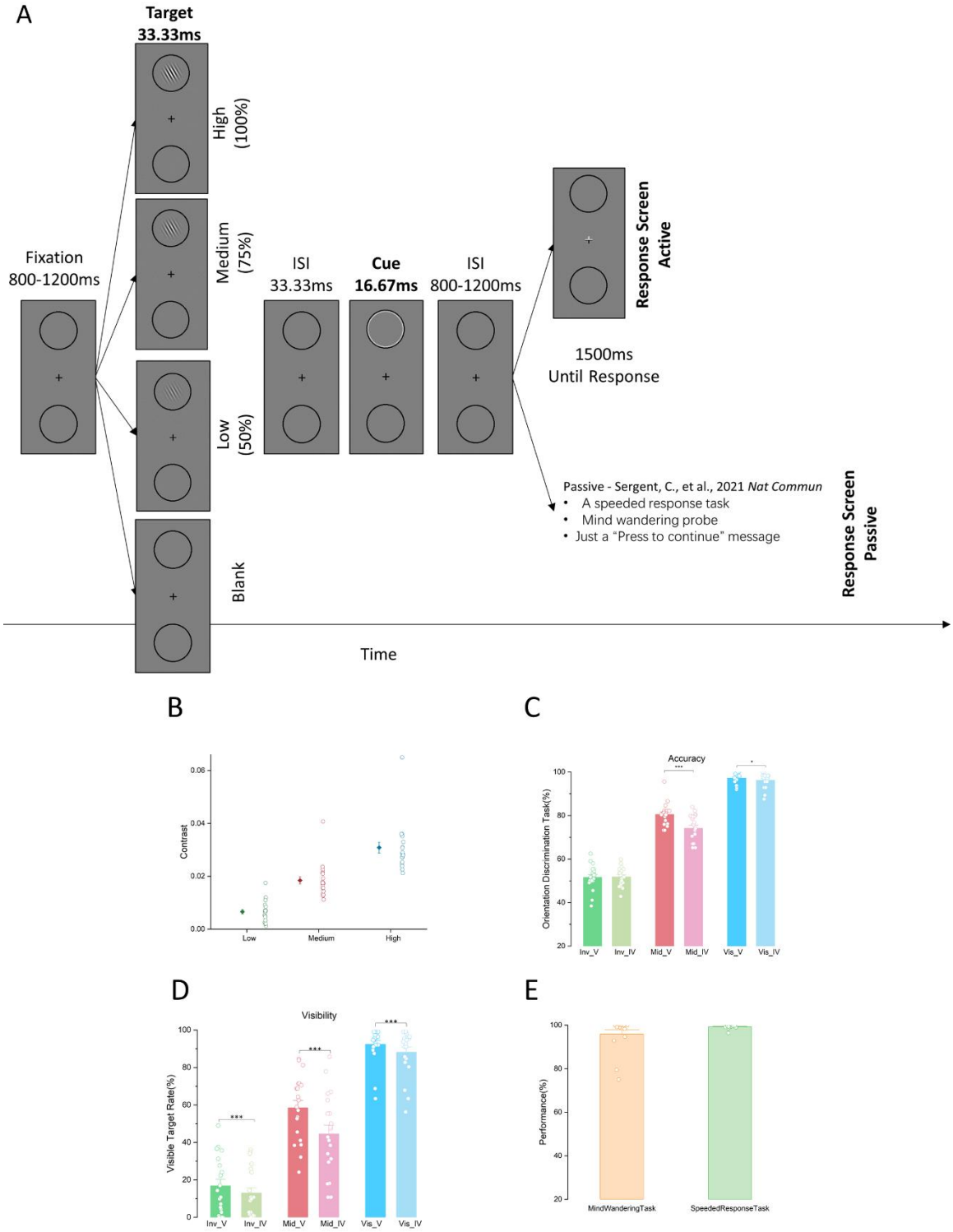

Figure 3. Experiment 3 Behavioral Results
(A) In Experiment 3, two circles were positioned above/below fixation. Gabor patches and cues randomly appeared in either circle, with stimulus intensity (high/medium/low contrast) calibrated via staircase tests to achieve ~100%, ~75%, and ~50% orientation discrimination accuracy,

respectively. Catch trials used Experiment 2's fixation screen. On active trials, participants simultaneously reported Gabor orientation (Left/Right) and subjective visibility (visible/invisible) via four response options. Passive trials required completing one of three randomized tasks: speed response, mind-wandering detection, or "Press SPACE to continue" prompts (details in Methods).

(B) Average contrast levels across three conditions. The x-axis displays the different Gabor patch contrasts (Low, Medium, and High), while the y-axis represents the contrast values. Dots on the right indicate individual contrast levels used to control orientation discrimination performance at 50%, 75%, and 100% accuracy. The graph illustrates the linear progression of contrast levels across the three conditions.

(C,D) C-Target Subjective Visibility in Experiment 3: Dots represent individual performance. The proportion of trials in which the target was visible is presented on the y-axis. The different Gabor patch contrasts (Invisible, Medium, and Visible) are presented on the x-axis. D-Target Orientation Discrimination 2AFC Task in Experiment 3: Dots represent individual performance, with the chance level at 50%. Accuracy is presented on the y-axis. The different target contrast conditions are presented on the x-axis.

(E) Performance on the Mind-Wandering Task and Speeded Response Task in the No-Report Condition. All error bars represent the standard error.

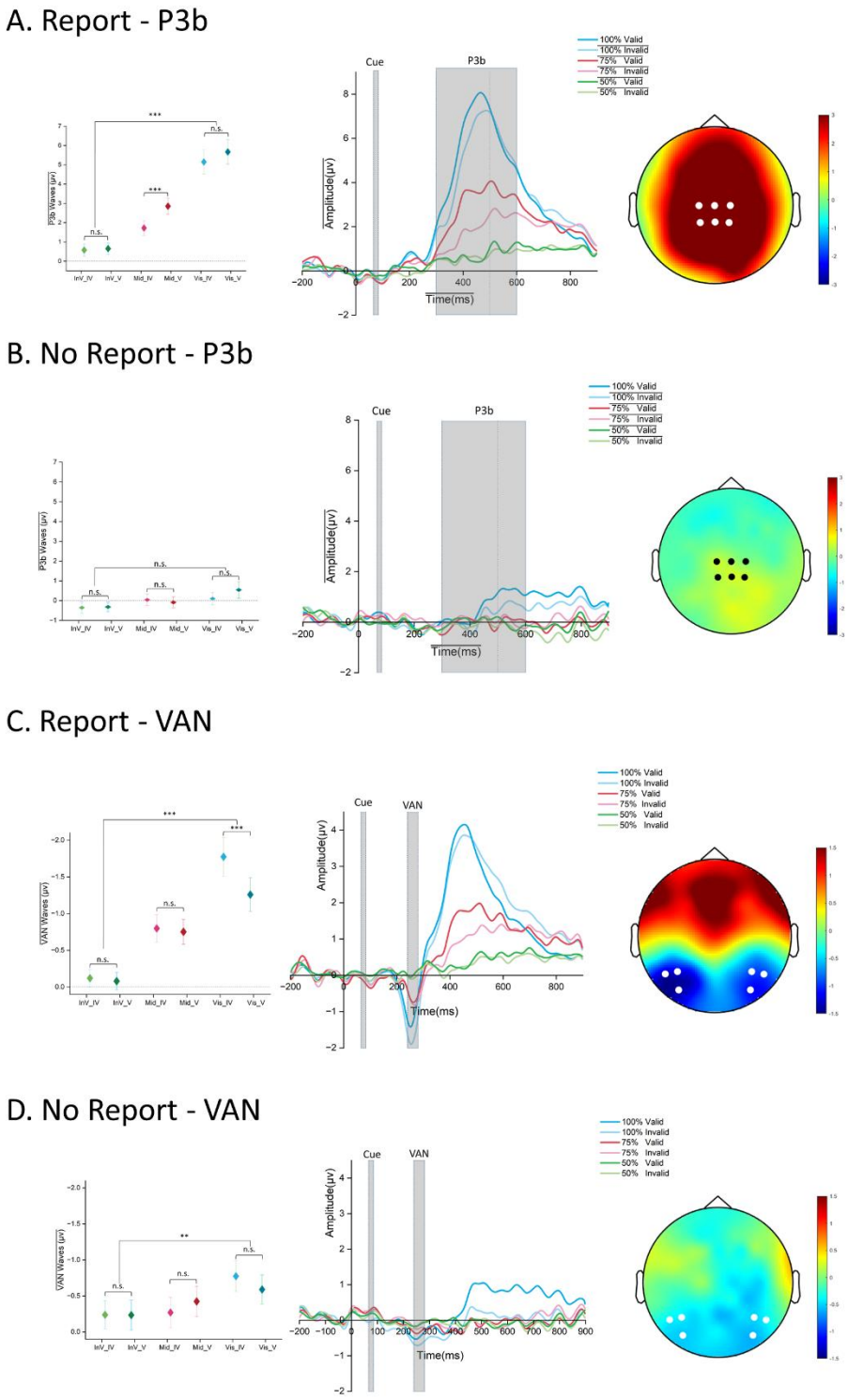

Figure 4. Experiment 3 ERP Results

(A,C) Report condition and (B,D) no-report condition. On the left: The average amplitudes from all electrodes used for the P3b (A,B) and VAN (C,D) across all six conditions. On the center: P3b and VAN waveforms for all six conditions (3 contrasts × 2 congruencies) plotted over time. On the right: Topographical voltage distributions between 300-600ms with all electrodes used to analyze the P3b and VAN indicated on the scalp map.

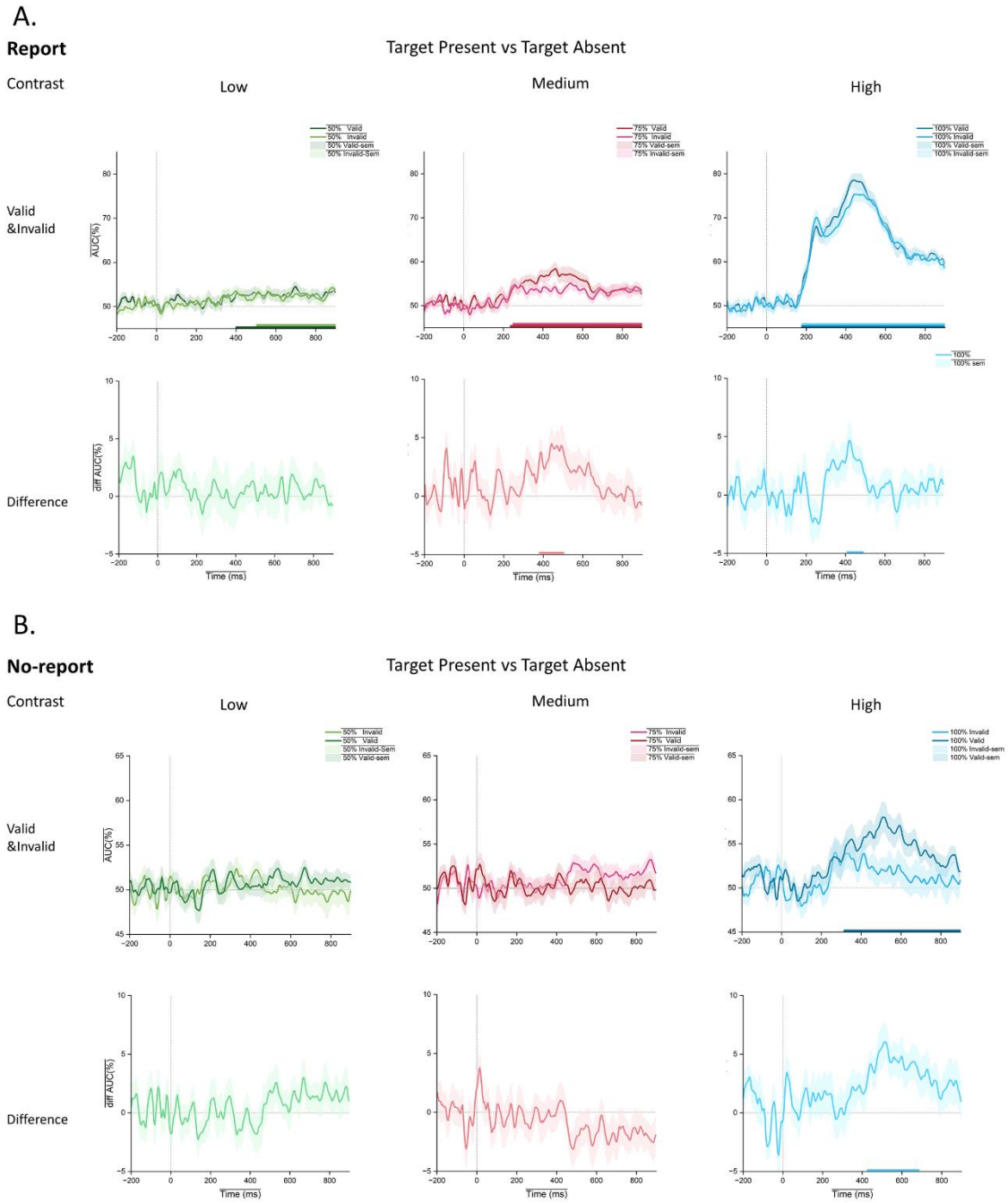

Figure 5. Experiment 3 Time Decoding Analysis Results

Decoding time courses in the report condition (A) and the no-report condition (B) (target present vs. target absent) were analyzed. All nine conditions (3 contrasts: 50%, 75%, 100% × 3 congruencies: valid, invalid, difference (valid-invalid)) were plotted, with decoding performance (AUC) shown as a function of time. The top row represents the valid and invalid condition, and the bottom row shows the difference: valid minus invalid condition. Color bars indicate significant clusters identified by cluster-based permutations, p corrected <0.05.

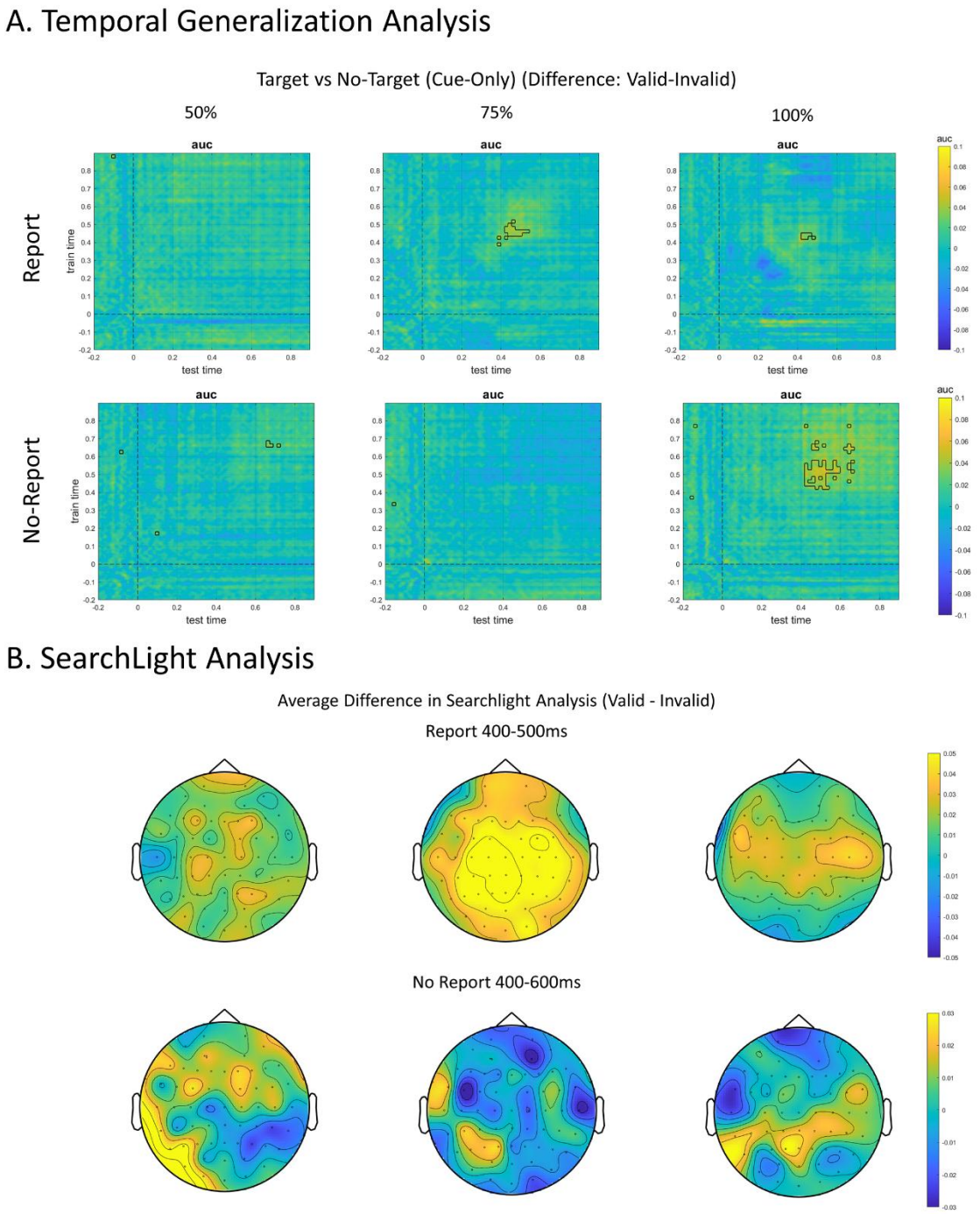

Figure 6. Experiment 3 Temporal Generalization & Search Light Analysis Results
(A) Searchlight Analysis results for the report condition (top) between 400 and 500ms and the no-report condition between 400 and 600ms. All six conditions (3 contrasts: 50%, 75%, 100% × difference (valid-invalid) × 2 (report no-report)) were plotted, with decoding performance (AUC) shown as a function of time. The top row represents the report condition, and the bottom row shows the no-report (All images display differences in decoding performances (valid – invalid)). Color bars indicate decoding performances.

(B) A decoder was trained to discriminate between target-present and target-absent trials from 0 to 900 ms. In the report condition and the no-report condition, all six conditions (3 contrasts: 50%, 75%, 100% × difference (valid-invalid)) × 2 (report no-report) with the decoding temporal generalization matrix (TGM). The top row represents the report condition, and the bottom row shows the no-report (All images display differences in decoding performances (valid – invalid)). Black contours indicate periods where classification deviated significantly from chance at p corrected < 0.01 (FDR).